Available online at www.sciencedirect.com
SCIENCE DIRECT®
Journal of the European Ceramic Society 25 (2005) 3287–3292
www.elsevier.com/locate/jeurceramsoc

Morphology of calcium phosphate coatings deposited on a Ti–6Al–4V substrate by an electrolytic method under 80 Torr

Szu-Hao Wang[a], Wei-Jen Shih[b], Wang-Long Li[a], Min-Hsiung Hon[b], Moo-Chin Wang[a,c,*]

[a] *Department of Mechanical Engineering, National Kaohsiung University of Applied Sciences, 415 Chien-kung Road, Kaohsiung 80782, Taiwan*
[b] *Department of Materials Science and Engineering, National Cheng Kung University, 1 Ta-Hsueh Road, Tainan 70101, Taiwan*
[c] *Department of Materials Engineering, National United University, 1 Lien-Da Road, Kung-ching Li, Miao Li 360, Taiwan*

Received 3 April 2004; received in revised form 12 August 2004; accepted 19 August 2004
Available online 28 October 2004

Abstract

Calcium phosphate coatings were deposited on the Ti–6Al–4V alloy plate in a 0.04 M $Ca(H_2PO_4)_2{\cdot}H_2O$ (MCPM) solution at 4–10 V, 0–60 °C, 1 h, and 80 Torr. X-ray diffractometry (XRD), scanning electron microscopy (SEM), energy dispersive spectrometry (EDS) and transmission electron microscopy (TEM) were used to identify the coating morphology and microstructure. Electrolytic deposition at 80 Torr improves the gathering of the bubbles on the cathode surface, and blocks the deposition of calcium phosphates. Under 80 Torr, the films are regularly interconnected at applied voltages greater than 7 V owing to rapid degassing. OH^- increases with increasing applied voltage. When excess OH^- is present, hydroxyapatite (HAP) is deposited on the Ti–6Al–4V substrate. The plate-like grains formed at applied voltages under 5 V are identified as dicalcium phosphate dehydrate (DCPD). HAP deposition occurs when the applied voltage is greater than 7 V. HAP increases with increasing electrolyte temperature.

Keywords: Films; Apatite; Biomedical applications; Microcrack toughening

1. Introduction

Biologically relevant calcium phosphates involve amorphous calcium phosphate (ACP), brushite (DCPD), monetite (MCP), octacalcium phosphate (OCP), tricalcium phosphate (TCP), calcium pyrophosphate and apatite.[1] In 1926, De Jong,[2] using X-ray diffraction (XRD) and chemical analysis, first identified the mineral phase of dentine, enamel and bone as calcium phosphate with an apatite structure similar to, and idealized to hydroxyapatite (HAP), $Ca_{10}(PO_4)_6(OH)_2$. The biocompatibility of hydroxyapatite is great, but with poor mechanical properties especially brittleness. However, a Ti–6Al–4V alloy often offers better mechanical properties. Coating bioactive ceramics onto Ti–6Al–4V substrate is therefore a popular method to provide metals with bone-bonding ability.

Since the bioenvironment in the human body is very complicated, metallic implants could interact with surrounding tissues and then cause corrosion. Clinical experience has shown that they are susceptible to localized corrosion in human bodies causing the release of metal ions into the tissues surrounding the implants. So biocompatible and corrosion-resistant layers are normally coated on alloys. Many efforts have been made in recent years in the development of processing methods for depositing HAP on implant alloy substrates such as Ti–6Al–4V in order to have high strength, suitable specific density, good process ability, and excellent corrosion resistance in living bodies.

There are numerous methods to deposit HAP layers on metallic devices, such as plasma-spraying,[3,4] electrophoretic methods[5,6] and electrochemical methods. Electrochemical methods for calcium phosphate coatings for biomedical applications have been investigated since the 1990s.[7–11] Calcium phosphate coatings have been deposited on various metal substrates by an electrochemical method, which is

* Corresponding author. Tel.: +886 37 381710; fax: +886 37 324047.
E-mail address: mcwang@nuu.edu.tw (M.-C. Wang).

0955-2219/$ – see front matter © 2004 Elsevier Ltd. All rights reserved.
doi:10.1016/j.jeurceramsoc.2004.08.016

an attractive process because highly irregular objects can be coated relatively quickly at low temperatures, and the coating morphology can be controlled by varying electrochemical potential, current density, electrolyte concentration and temperature.[12] When the electrolyte contains Ca^{2+} and $H_2PO_4^{1-}$, it will produce calcium phosphate powders, such as MCP, DCPD, OCP, ACP, HAP.[13,14] Among them, HAP is the most interesting form of calcium phosphate to be electrochemically deposited from several solutions at elevated temperatures.[15–19] In this study, the electrolyte has only one source powder, monocalcium phosphate monohydrate (MCPM), so the composition of the films is formed from calcium phosphates only, such as DCPD, ACP and HAP, which are found in chemical synthesis without amino or chlorine compounds.

The main objective of this study is to investigate the morphology of calcium phosphate coatings deposited on a Ti–6Al–4V substrate at different temperatures and applied voltages by electrolysis in 0.04 M $Ca(H_2PO_4)_2{\cdot}H_2O$ aqueous solution under 80 Torr for 1 h.

2. Experimental procedure

2.1. Sample preparation

This study used a Ti–6Al–4V alloy plate as a cathode and a platinum plate as anode. The composition of the Ti–6Al–4V alloy plate conformed to the specification of ASTM standard F-136. The Ti–6Al–4V alloy plate with a size of 15 mm × 15 mm × 3 mm was mechanically ground with SiC papers from 120 to 1200 grit and polished with 0.3 μm Al_2O_3 powders to a mirror finish. The Ti–6Al–4V plate was then washed thoroughly by running distilled water before being ultrasonically degreased with acetone and dried at 60 °C.

2.2. Electrolytic deposition

The saturated 0.04 M electrolyte was prepared by adding 1 g monocalcium phosphate monohydrate ($Ca(H_2PO_4)_2{\cdot}H_2O$, analytical grade, Showa Chemical Co. Ltd., Tokyo, Japan) in 100 ml deionized water. The electrolyte was stirred with a magnetic stirrer for 1 h to enhance the dissolution of the calcium phosphate. The pH of the electrolyte was about 3.0. Electrolysis was carried out at a cathode voltage and temperature of 4–10 V and 0–60 °C, respectively, for 60 min. The distance between the electrodes was 3 cm and the cathode area was maintained at 1.057 cm^2. The ambient pressure of 80 Torr was selected for the electrolysis to improve the bubbles assembling in the vicinity of the cathode surface (Ti–6Al–4V substrate). The diagram of apparatus was shown in Fig. 1. After deposition, the sample was washed in distilled water and dried at room temperature.

2.3. Sample characterization

The crystalline composite phases of the dried sample were examined with XRD (Rigaku D-Max/IIIV, Tokyo, Japan). A monochromatic Cu Kα radiation was selected (λ = 1.54052 Å). The operation tube voltage and current were 30 kV and 20 mA, respectively. The scanning angle of the sample was from 20° to 55° with a scanning speed of 4°/min. The coating microstructure and morphology were studied with scanning electron microscopy (Hitachi S2700 SEM, Tokyo, Japan). In addition, the Ca/P ratio was determined with an energy dispersive spectrometer (EDS, AN10000/855, LINKS, England). The sample preparation was carried out by dispersing powders in an ultrasonic bath and then collected on a copper grid.

A transmission electron microscope was used to recognize the crystal structure (Hitachi HF-2000 Field Emission Transmission Electron Microscope, HF-2000, Tokyo, Japan) under 200 kV.

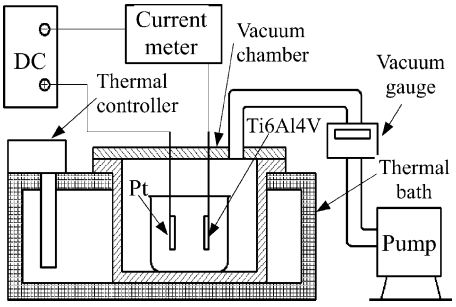

Fig. 1. Diagram of low pressure electrochemical deposition apparatus.

3. Results and discussion

Fig. 2 shows the specimen deposited at 7 V under normal atmospheric pressure and 80 Torr at 30 °C for 1 h. Under the normal atmospheric pressure, the deposit on the Ti–6Al–4V substrate is irregular and flakes off due to bubbles gathering at the cathode surface. Bubbles quickly lift up from the cathode surface at 80 Torr and the deposit is regular and integrated.

Elmore and Farr[20] studied the dissolution of $Ca(H_2PO_4)_2{\cdot}H_2O$ (MCPM) at temperatures from 25 to 100 °C and reported the following reactions:

$$Ca(H_2PO_4)_2 \cdot H_2O + xH_2O \xrightarrow{H_2O} CaHPO_4 + H_3PO_4 + (1+x)H_2O \quad (1)$$

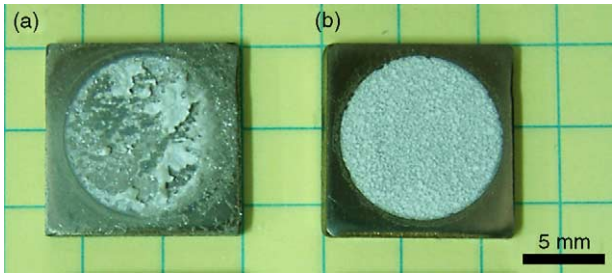

Fig. 2. Specimens deposited at 7 V under (a) normal atmosphere pressure and (b) 80 Torr at 30 °C for 1 h.

H_3PO_4 is stepwise dissociated, so that $H_2PO_4^{1-}$, HPO_4^{2-} and PO_4^{3-} ions exist at the electrode. The other related cathode reactions[21] are as follows:

$$2H_2O + 2e^- \rightarrow H_2 + 2OH^- \quad (2)$$

$$2H_2PO_4^{1-} + 2e^- \rightarrow 2HPO_4^{2-} + H_2 \quad (3)$$

$$2HPO_4^{2-} + 2e^- \rightarrow 2PO_4^{3-} + H_2 \quad (4)$$

Dicalcium phosphate dehydrate ($CaHPO_4{\cdot}2H_2O$, DCPD) is formed on the cathode surface as expressed by the following reaction (5):

$$Ca^{2+} + HPO_4^{2-} + 2H_2O \rightarrow CaHPO_4 \cdot 2H_2O \quad (5)$$

It has been established that the electrolytic deposition results in an increasing pH at the interface due to electron incorporation to form OH^- ions and H_2 through water reduction.[22] Many bubbles and OH^- ions are produced around the cathode electrode with increasing applied voltage. OH^- diffuses rapidly in the electrolyte and causes the pH change around the metal/solution interface.[14] When excess OH^- (reaction (2)) is produced, HAP can be deposited on the cathode surface by the following reaction (6):

$$10Ca^{2+} + 6PO_4^{3-} + 2OH^- \rightarrow Ca_{10}(PO_4)_6 \cdot (OH)_2 \quad (6)$$

When pH value is low, the HPO_4^{2-} ion is stable, hence the reactions (3) and (5) are the major reaction. When pH value became higher for the OH^- around the metal/solution interface, PO_4^{3-} ion is more stable, and the reactions (4) and (6) dominate.[23]

H_2 gas is produced in reactions (2), (3) and (4). The reaction becomes intense when the applied voltage is increased. The bubbles assembled in the vicinity of the cathode surface inhibit the calcium phosphate formation and its deposition on the Ti–6Al–4V alloy substrate.

The XRD patterns of the deposited coatings at 60 °C are shown in Fig. 3. All diffraction peaks are assigned to the crystalline DCPD (JCPDS card number 72-1240), HAP (JCPDS card number 09-9432) and Ti (JCPDS card number 44-1294). The thickness of the deposits becomes greater as the applied voltage increases, and induces reduced substrate reflections at $2\theta = 37.8°$ and 39.6°. DCPD is the major phase of the films deposited at the applied voltages of 4 and 5 V. When the applied voltage is 4 V, the deposit is sparse, so the DCPD peak is weak in Fig. 3a. The intensity of the DCPD (0 4 0) peak at $2\theta = 22.8°$ is irregularly strong and gradually decreases with increasing applied voltage. In the SEM observation, the size of the plate-like DCPD gradually decreases and then vanishes as the applied voltage rises. So the plate-like DCPD would have the (0 4 0) preferred orientation. When the applied voltage is increased to 7 V (Fig. 3c), DCPD is still the major phase, but the HAP reflections increase relatively. However, the pattern illustrates clearly the HAP (0 0 2) peak at $2\theta = 25.88°$ and the broadened HAP (2 1 1) peak at $2\theta = 31.77°$. When the applied voltage is raised to 10 V (Fig. 3d), DCPD is dramatically decreased and HAP becomes the main substance.

Fig. 4 shows the XRD patterns of the specimens deposited at 7 V in the electrolyte at 0, 30 and 60 °C under 80 Torr for 1 h. The thickness of the deposits becomes greater as the temperature increases, and induces the decreasing of the titanium alloy reflections. The diffraction peaks due to the DCPD and HAP phases are observed in the patterns for the applied voltage of 7 V at 0 to 60 °C. The intensity of the peaks of HAP at 60 °C (Fig. 4c) is significantly higher than those at 0 °C (Fig. 4a) and 30 °C (Fig. 4b), which reveals an increase of HAP and a decrease of DCPD with temperature. It is known that the solubility of calcium phosphate decreases with solution temperature. The relationship between solubility product, k_s, and solution temperature, T, for hydroxyapatite is given by Elliot.[24]

$$\log k_s = -\frac{82194.4}{T} - 1.6657 - 0.09825T \quad (7)$$

Ban and Hasegawa[25] have found that the crystal growth of HAP increases with increasing electrolyte temperature.

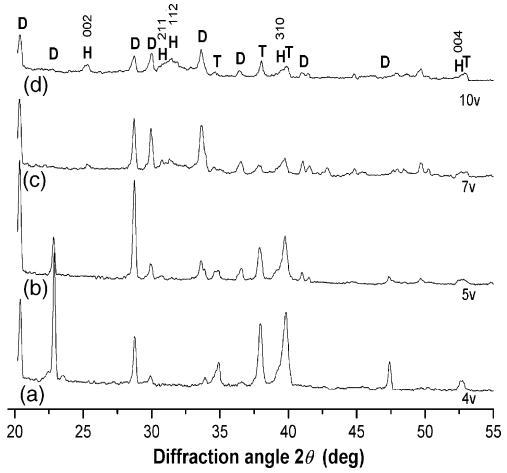

Fig. 3. XRD patterns of the specimens deposited under 80 Torr at 60 °C: (a) 4 V, (b) 5 V, (c) 7 V, and (d) 10 V for 1 h. H:HAP, T:Ti, D:DCPD.

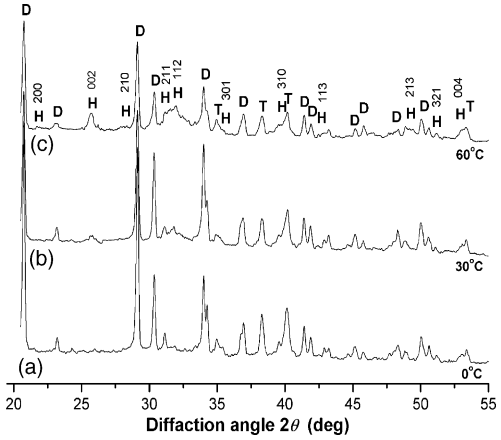

Fig. 4. XRD patterns of the specimens deposited under 80 Torr at 7 V: (a) 0 °C, (b) 30 °C, and (c) 60 °C for 1 h. H:HAP, T:Ti, D:DCPD.

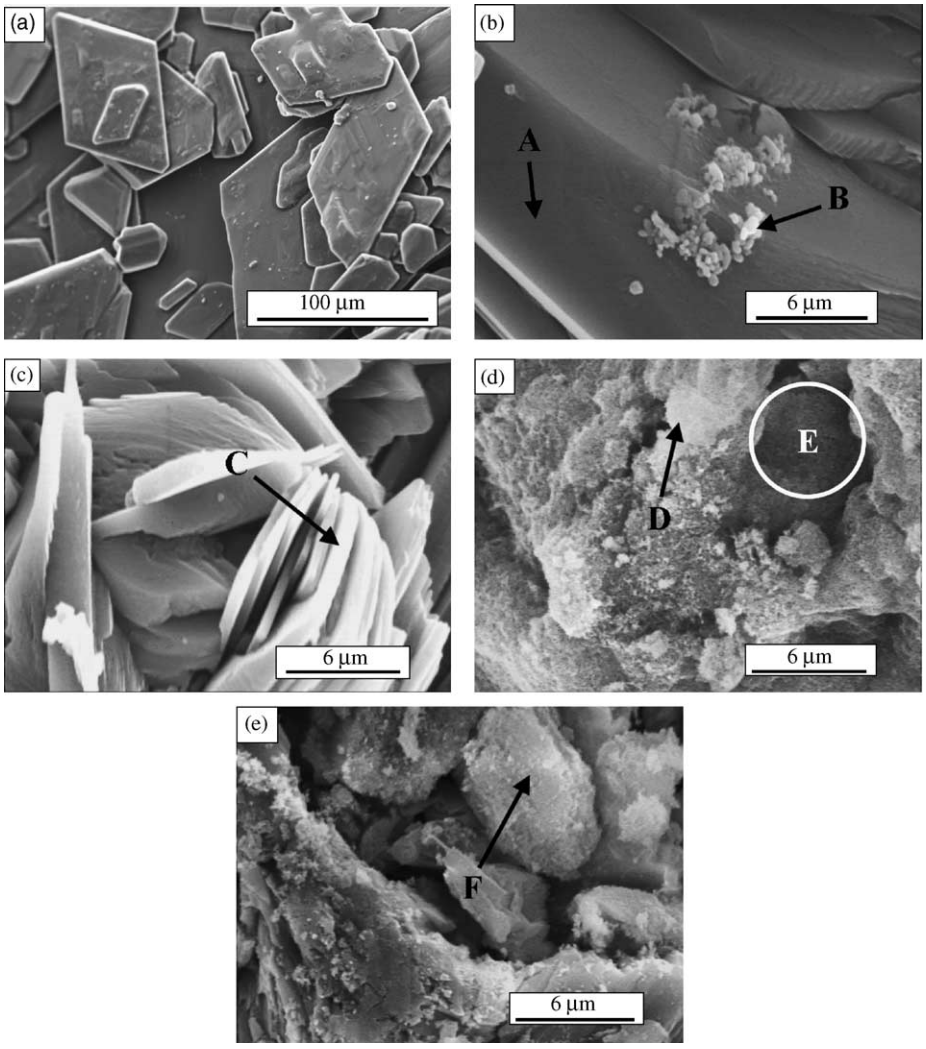

Fig. 5. SEM images of (a) starting material, MCPM and specimens deposited under 80 Torr at 60 °C for 1 h (b) 4 V, (c) 5 V, (d) 7 V, and (e) 10 V.

Additionally, the broadened peaks of HAP reveal a coating with poor crystallinity or composed of small crystallites, which being similar to natural bone mineral, are suitable for tissue compatibility.[26]

The SEM micrograph (Fig. 5a) reveals flat, triclinic MCPM in the starting material with a typical size of 100 μm in length. Fig. 5b–e shows SEM micrographs of the deposits on the Ti–6Al–4V substrate under 4, 5, 7 and 10 V in the electrolyte at 60 °C. Plate-like precipitates are observed in the specimen with the applied voltage of 5 V (Fig. 5c). The width and length of the plates at 4 V (Fig. 5b) are larger than

Table 1
EDS analysis at the different locations in Fig. 5

Applied voltage (V)	Morphology at different locations	Chemical composition (at.%)			Ca/P ratio
		Ca	P	O	
4	Plate-like at A	23.96	22.00	54.04	1.089
	Particles at B	20.44	18.59	60.97	1.100
5	Plate-like at C	24.69	23.38	51.93	1.056
7	Granular at D	39.42	23.33	37.25	1.690
	Needle-like at E	23.80	16.18	60.02	1.471
10	Granular at F	33.99	22.11	43.90	1.537

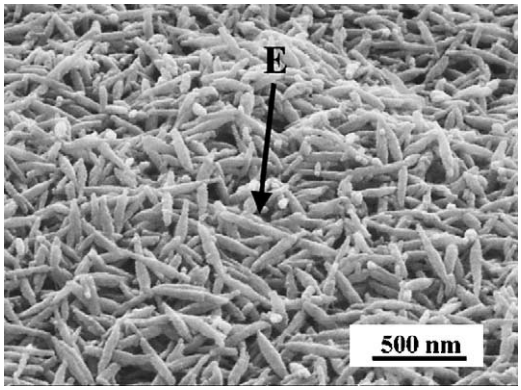

Fig. 6. Magnified SEM image of **E** in Fig. 5d.

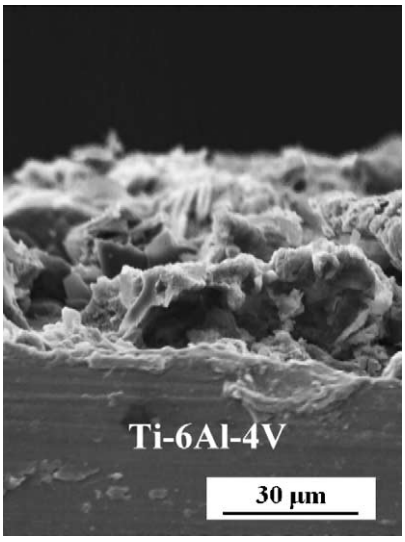

Fig. 7. Cross-sectional view of the specimens deposited under 80 Torr at 60 °C with 10 V for 1 h.

those at 5 V. The compositions of the species with various morphologies marked from A to E are identified by EDS in Table 1. Granular (D) and needle-like (E) precipitates are observed at applied voltages over 7 V.

Fig. 6 shows the SEM micrograph of the needle-like specimen deposited at 60 °C with 7 V. The width and length of the needles are about 60 and 300 nm, respectively. The needle-like substance is identified as $Ca_3(PO_4)_2{\cdot}nH_2O$ (ACP) by EDS.

Fig. 7 shows the SEM micrograph of the cross-section of the deposit at 60 °C under 10 V for 1 h. The image shows a macroporous calcium phosphate layer on the Ti–6Al–4V substrate. Such a bioactive macroporous layer on an implant is expected not only to enhance bony ingrowth into the porous structure, but also to provide a chemical integration with bone via apatite formation on its surface in the body.[27]

The EDS results of the different deposits are listed in Table 1. When the applied voltage is under 5 V, the plate-like substance has a Ca/P ratio of about 1.0. According to its XRD study, it is identified as DCPD. The needle-like aggregates appear at applied voltages over 7 V with Ca/P ratios close to 1.50, which is identified as ACP. The HAP phase appears when the applied voltage is over 7 V in Fig. 3, and the Ca/P ratio of the granular structure is close to 1.67.

The TEM image of the specimen deposited at 60 °C and 4 V under 80 Torr for 1 h is shown in Fig. 8. In Fig. 8a, the crystal has a lath-like shape with 30 nm width and 250 nm length. Occasionally, discontinuous or weak ring patterns are

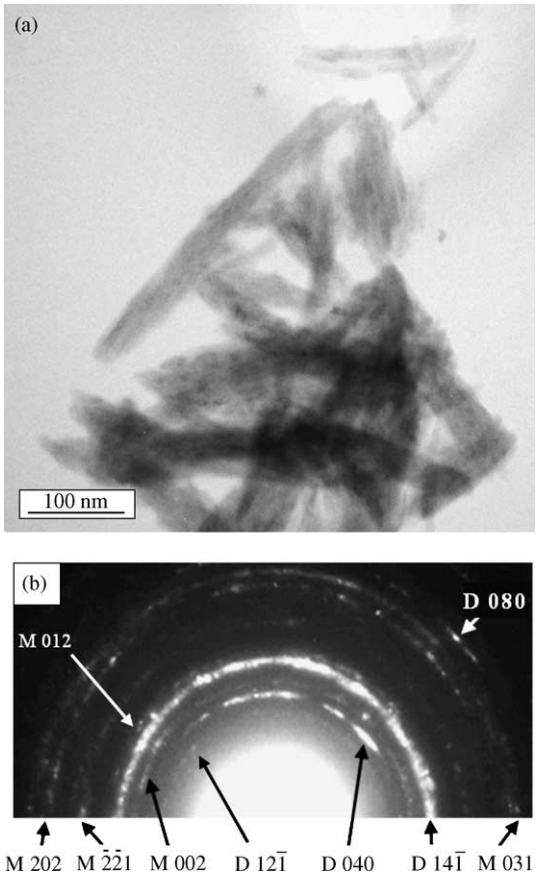

Fig. 8. TEM image and ED pattern of the calcium phosphate deposited on the Ti–6Al–4V alloy at 60 °C, 4 V for 1 h: (a) BF image and (b) ring pattern, index corresponding to phase of DCPD and MCP.

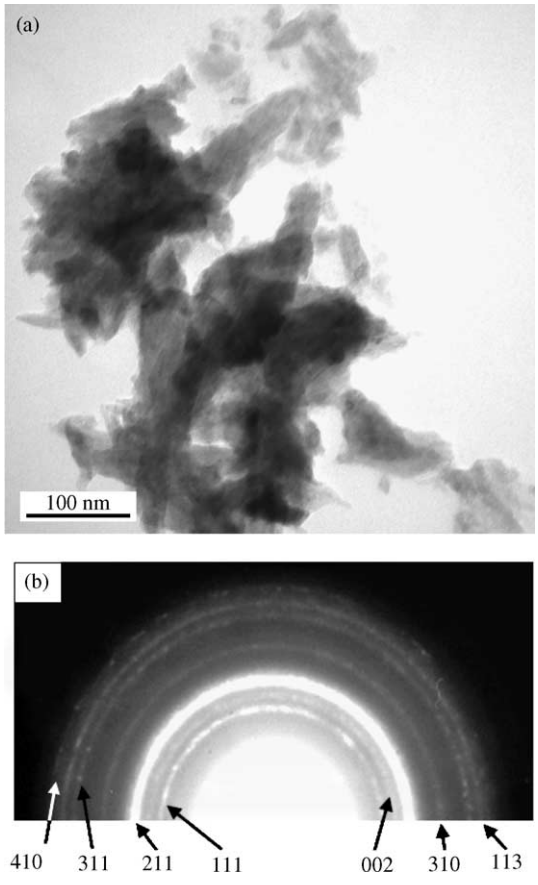

Fig. 9. TEM image and ED pattern of the calcium phosphate deposited on the Ti–6Al–4V alloy at 60 °C, 10 V for 1 h: (a) BF image and (b) ring pattern, index corresponding to phase of HAP.

shown in Fig. 8b, which results from the diffraction of DCPD and MCP nanosized crystallites. In Fig. 3a, only DCPD is found and there is no d-spacing of HAP, corresponding to the ring patterns.[28]

Fig. 9 shows the TEM micrograph of the specimen deposited at 60 °C and 10 V under 80 Torr for 1 h. In Fig. 9a, the crystal has a rod-like shape with 50 nm width and 150 nm length with rough edges. Fig. 9b shows the corresponding diffraction ring pattern of the HAP polycrystals. With the XRD study, the products are identified to be the DCPD and HAP phases and no other calcium phosphates are found.

4. Conclusions

Electrolytic deposition at 80 Torr improves bubble removal in the vicinity of the cathode surface and encourages the deposition of calcium phosphates. The films are regular and interconnected at applied voltages greater than 7 V under 80 Torr.

At 60 °C, the plate-like crystals formed at 5 V are identified to be DCPD; HAP occurs when the applied voltage is over 7 V. The electrolytic deposition product is essentially composed of amorphous calcium phosphate, $Ca_3(PO_4)_2{\cdot}nH_2O$ (ACP) at 5–7 V. The crystal growth of HAP increases with increasing electrolyte temperature. Different calcium phosphate phases are formed on substrates depending on applied voltage and electrolyte temperature.

Acknowledgements

The authors gratefully acknowledge the financial support and partial support by the National Science Council (NSC92-2216-E-151-007) and National Kaohsiung University of Applied Sciences (KUAS-ME-92001), Taiwan, Republic of China, and Pror. M.P. Hung for discussion in the manuscript preparation.

References

1. LeGeros, R. Z., *Calcium Phosphates in Oral Biology and Medicine, Karger*., 1991 (p. 82–107).
2. Prado Da Silva, M. H., Lima, J. H. C., Soares, G. A., Elias, C. N., de Andrade, M. C., Best, S. M. *et al.*, Transformation of monetite to hydroxyapatite in bioactive coatings on titanium. *Surf. Coatings Tech.*, 2001, **137**, 270–276.
3. Koch, B., Wolke, J. G. C. and De Groot, K., X-ray diffraction studies on plasma-sprayed calcium phosphate-coated implants. *J. Biomed. Mater. Res.*, 1990, **24**, 665–667.
4. Ellies, L. G., Nelson, D. G. and Featherstone, J. D., Crystallographic changes in calcium phosphate-coated implants. *Biomaterials*, 1992, **13**, 313–316.
5. Ducheyne, P., Radin, S., Heughebaert, M. and Heughebaert, J. C., Calcium phosphate ceramic coatings on porous titanium: effect of structure and composition on electrophoretic deposition, vacuum sintering and in vitro dissolution. *Biomaterials*, 1990, **11**, 244–254.
6. Zhitomirsky, I., Electrophoretic hydroxyapatite coatings and fibers. *Mater. Lett.*, 2000, **42**, 262–271.
7. Cook, S. D., Thomas, K. A., Kay, J. F. and Jarcho, M., Hydroxyapatite-coated titanium for orthopedic implant applications. *Clin. Orthop. Relat. Res.*, 1988, **232**, 225–243.
8. De Groot, K., Geesink, R., Klein, C. P. A. T. and Serekian, P., Plasma aprayed coatings of hydroxylaptite. *J. Biomed. Mater. Res.*, 1987, **21**, 1375–1381.
9. Weng, J., Liu, Q., Wolke, J. G. C., Zhang, X. and De Groot, K., Formation abd characteristics of the apatite layer on plasma-sprayed hydroxyapatite coatings in simulated body fluid. *Biomaterials*, 1997, **18**, 1027–1035.
10. Lin, J. H. C., Liu, M. L. and Ju, C. P., Structure and properties of hydroxyapatite-bioactive glass composites plasma sprayed on Ti_6Al_4V. *J. Mater. Sci.: Mater. Med.*, 1994, **28**, 279–283.
11. Wolke, J. G. C., Van der Waerden, J. P. C. M., De Groot, K. and Jansen, J. A., *Biomaterials*, 1997, **18**, 483.
12. Ding, S. J., Ju, C. P. and Lin, J. H. C., Immersion behavior of RF magnetron-assisted sputtered hydroxyapatite/titanium coatings in simulated body-fluid. *J. Biomed. Mater. Res.*, 1999, **47**, 551–563.
13. DacuIsi, G., Biphasic calcium phosphate concept applied to articial bone, implant coating and injectable bone substitute. *Biomaterials*, 1998, **19**, 1473–1478.
14. Zhang, J. M., Lin, C. J., Feng, Z. D. and Tian, Z. W., Mechanistic studies of electrodeposition for bioceramic coatings of calcium phosphates by an in stiu pH-microsensor technique. *J. Electroanal. Chem.*, 1998, **452**, 235–240.
15. Shirkhanzadeh, M., Bioactive calcium phosphate coating prepared by electrodeposition. *J. Mater. Sci. Lett.*, 1991, **10**, 1415–1417.
16. Vijayaraghavan, T. V. and Bensalem, A., Electrodeposition of apatite coating on pure titanium and titanium alloys. *J. Mater. Sci. Lett.*, 1994, **13**, 1782–1785.
17. Ban, S. and Maruno, S., Effect of temperature on electrochemical deposition of calcium phosphate coatings in a simulated body fluid. *Biomaterials*, 1995, **16**, 977–981.
18. Shirkhanzadeh, M., Direct formation of nanophase hydroxyapatite on cathodically polarized electrodes. *J. Mater. Sci.: Mater. Med.*, 1998, **9**, 67–72.
19. Shirkhanzadeh, M. and Azadegan, Hydroxyapatite particles prepared by electrocrystallisation from aqueous electrolytes. *J. Mater. Lett.*, 1993, **15**, 392–395.
20. Elmore, K. L. and Farr, T. D., Equilibrium in the system calcium oxide–phosphorus pentoxide–water. *Ind. Eng. Chem.*, 1940, **32**, 580–586.
21. Jinawath, S., Pongkao, D., Suchanek, W. and Yoshimura, M., Hydrothermal synthesis of monetite and hydroxyapatite from monocalcium phosphate monohydrate. *Inter. J. Inorg. Mater.*, 2001, **3**, 997–1001.
22. Mansol, M., Jiménez, G., Morant, C., Herrero, P. and Maetínez-Duart, J. M., Electrodeposition of hyardoxaptite coating in basic conditions. *Biomaterials*, 2000, **21**, 1755–1761.
23. De Aza, P. N., Guitian, F., Merlos, A., Lora-Tamayo, E. and De Aza, S., Bioceramics-simulate body fluid interfaces: pH and its influence of hydroxyapatite formation. *J. Mater. Sci.: Mater. Med.*, 1996, **7**, 399–402.
24. Elliot, J. C., *Structure-Chemistry of Apatites and Other Calcium Orthophosphates*. Elsevier, Amsterdam, 1994 (p. 157).
25. Ban, S. and Hasegawa, J., Morphological regulation and crystal growth of hydrothermal-electrochemically deposited apatite. *Biomaterials*, 2002, **23**, 2965–2972.
26. Kuo, M. C. and Yen, S. K., The process of electrochemical deposited hydroxyapatite coating on biomedical titanium at room temperature. *Mater. Sci. Eng. C*, 2002, **20**, 153–160.
27. Kim, H. M., Kokubo, T., Fujibayashi, S., Nishiguchi, S. and Nakamura, T., Bioactive macroporous titanium surface layer on titanium substrate. *J. Biomed. Mater. Res.*, 2000, **52**, 553–557.
28. Leng, Y., Chen, J. and Qu, S., TEM study of calcium phosphate precipitation on HA/TCP ceramics. *Biomaterials*, 2003, **24**, 2125–2131.